Supplementary Information (SI) for Inorganic Chemistry Frontiers.

Electrocatalytic Hydrogen Evolution and Doping Modification of Weyl Semimetal $PtBi_2$ Acidic Solution

Yinghui Liu[a], Chen Qiubo[b], Yukai An[c], Hailong Qiu*[a], Shihui Ma*[a], Hongjun Liu[a], Zhanggui Hu[a] and Yicheng Wu[a]

Supporting Information

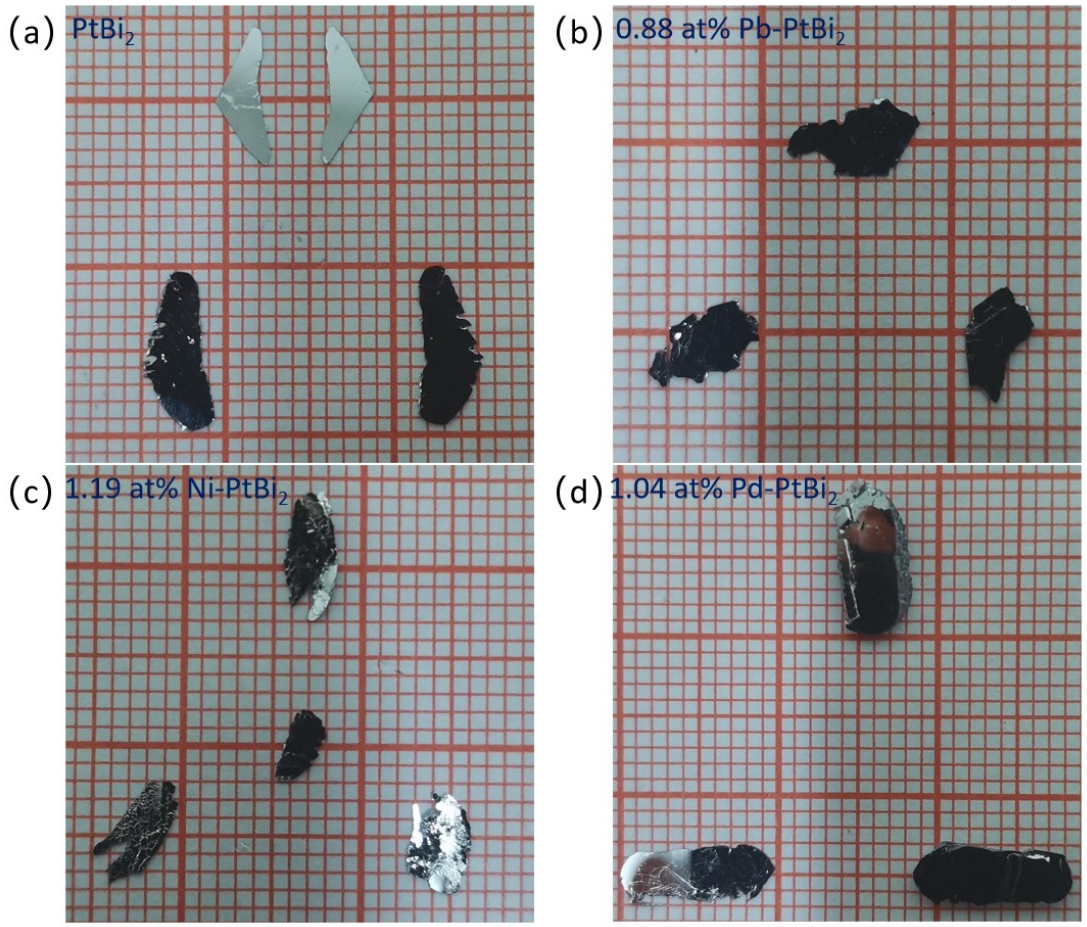

Fig. S1. Morphology and size of $PtBi_2$, 0.88 at% Pb-$PtBi_2$, 1.19 at% Ni-$PtBi_2$, and 1.04 at% Pd-$PtBi_2$ crystals grown using the self flux method.

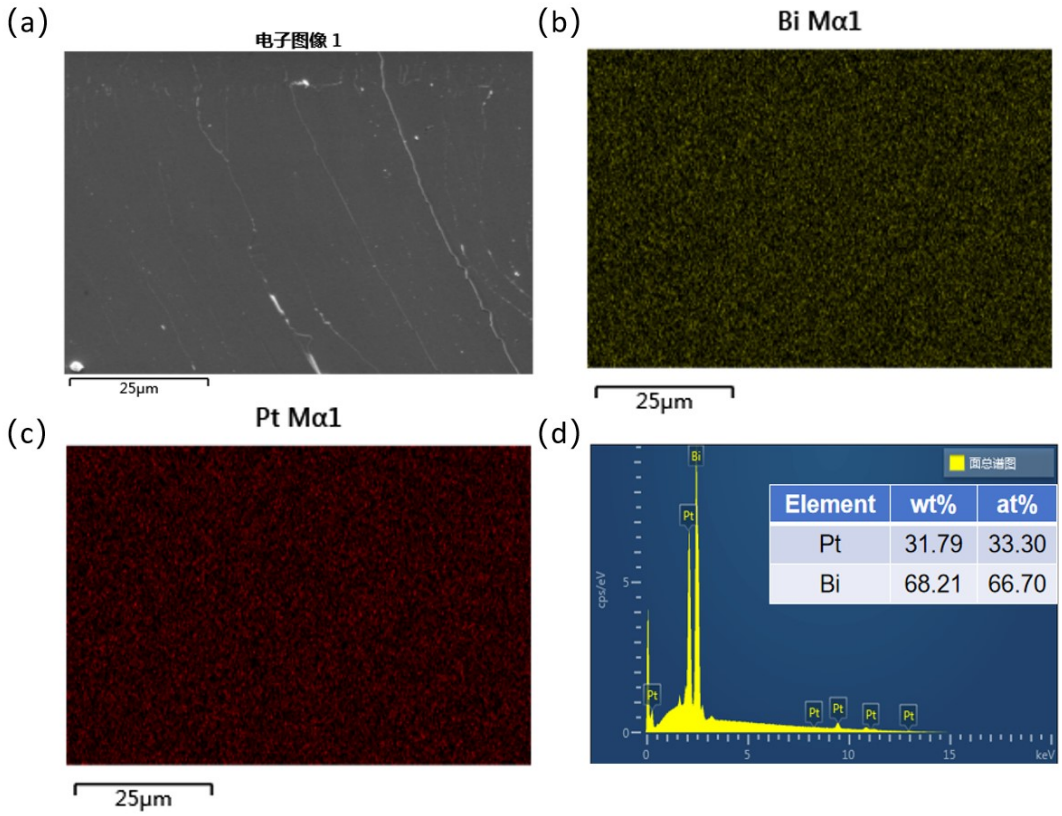

Fig. S2. SEM images of $PtBi_2$. EDX spectra of the Pt, Bi elements, and the quantification. Elemental analysis showing the distribution of Bi and Pt elements.

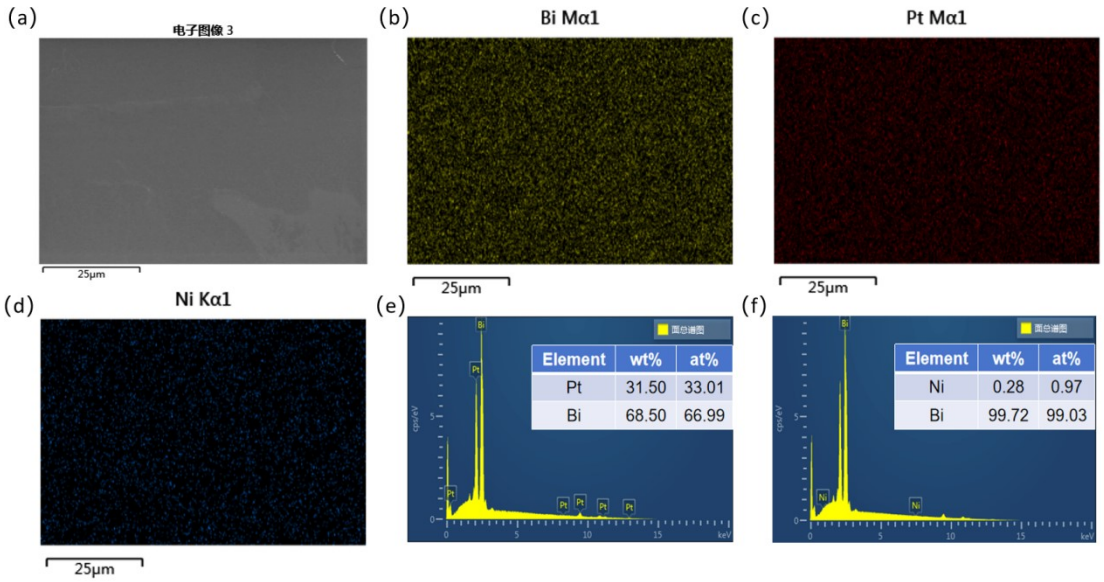

Fig. S3. SEM images of 0.65 at% Ni-$PtBi_2$. EDX spectra of the Pt, Bi elements, and the quantification.EDX spectra of the Ni, Bi elements and the quantification. Elemental analysis showing the distribution of Bi, Pt, and Ni elements.

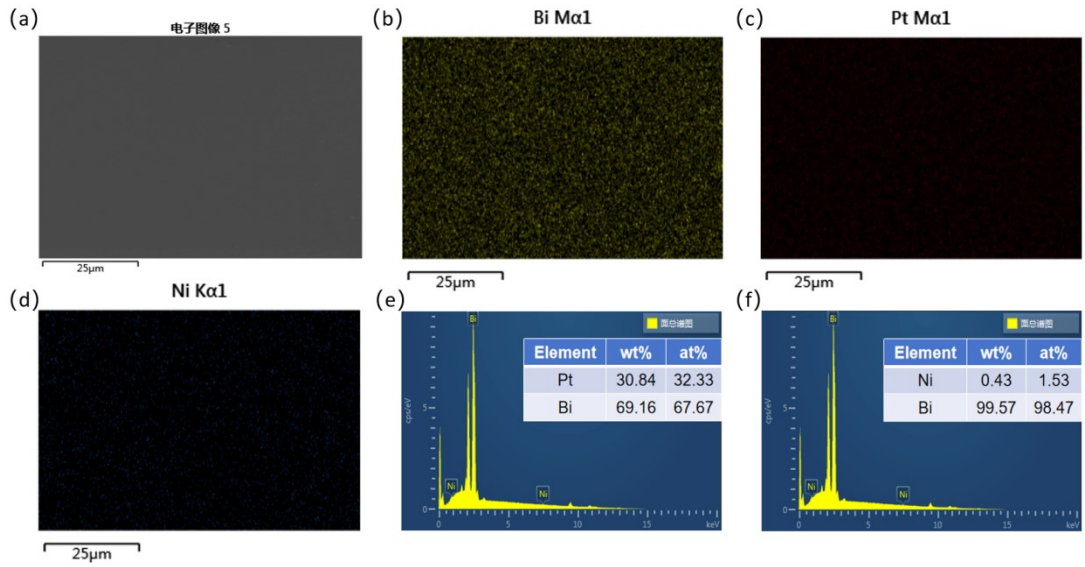

Fig. S4. SEM images of 1.04 at% Ni-$PtBi_2$. EDX spectra of the Pt, Bi elements, and the quantification. EDX spectra of the Ni, Bi elements and the quantification. Elemental analysis showing the distribution of Bi, Pt, and Ni elements.

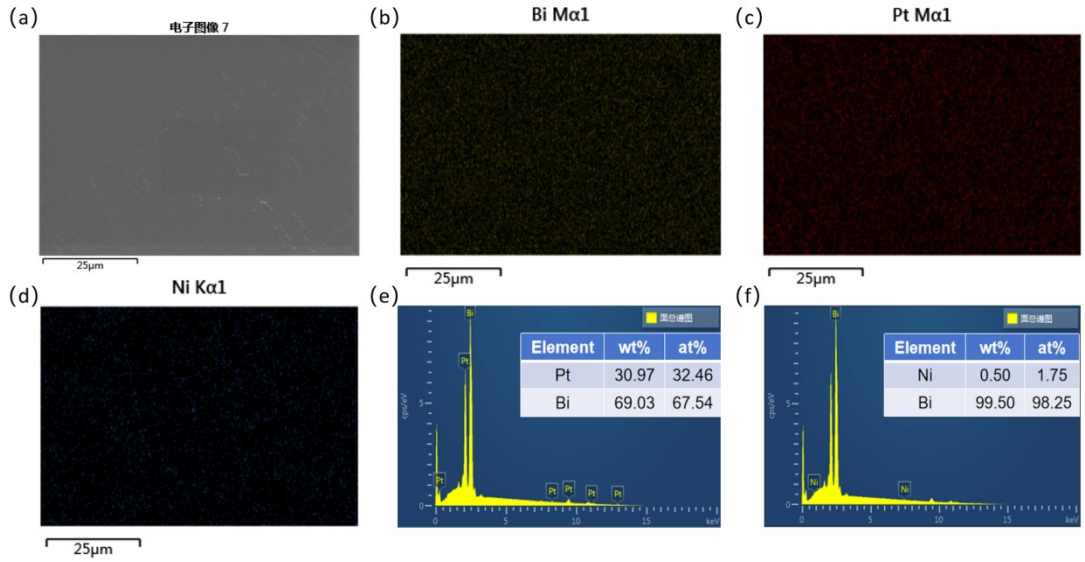

Fig. S5. SEM images of 1.19 at% Ni-$PtBi_2$. EDX spectra of the Pt, Bi elements, and the quantification.EDX spectra of the Ni, Bi elements and the quantification. Elemental analysis showing the distribution of Bi, Pt, and Ni elements.

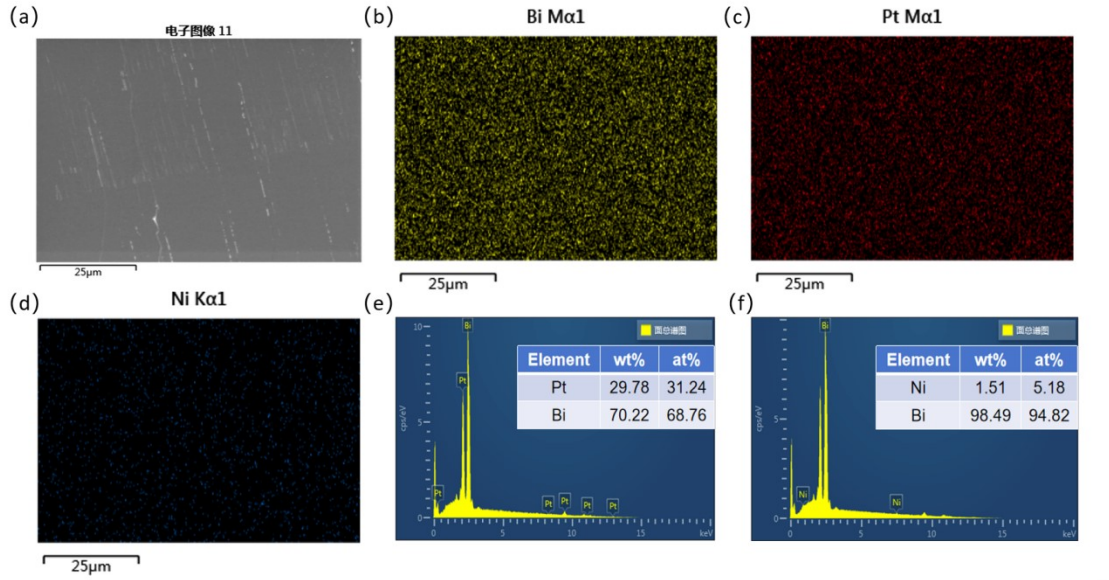

Fig. S6. SEM images of 3.62 at% Ni-$PtBi_2$. EDX spectra of the Pt, Bi elements, and the quantification.EDX spectra of the Ni, Bi elements and the quantification. Elemental analysis showing the distribution of Bi, Pt, and Ni elements.

Table S1: EDS test atomic ratios and calculated Ni atom occupancies for Ni doped crystals.

Label	Calculated Atomic Ratio Ni : (Ni+Pt+Bi)	EDS Test Atomic Ratio Pt : Bi	EDS Test Atomic Ratio Ni : Bi
0.65 at% Ni-$PtBi_2$	0.0065	33.01 : 66.99	0.97 : 99.03
1.04 at% Ni-$PtBi_2$	0.0104	32.33 : 67.67	1.53 : 98.47
1.19 at% Ni-$PtBi_2$	0.0119	32.46 : 67.54	1.75 : 98.25
3.62 at% Ni-$PtBi_2$	0.0362	31.24 : 68.76	5.18 : 94.82

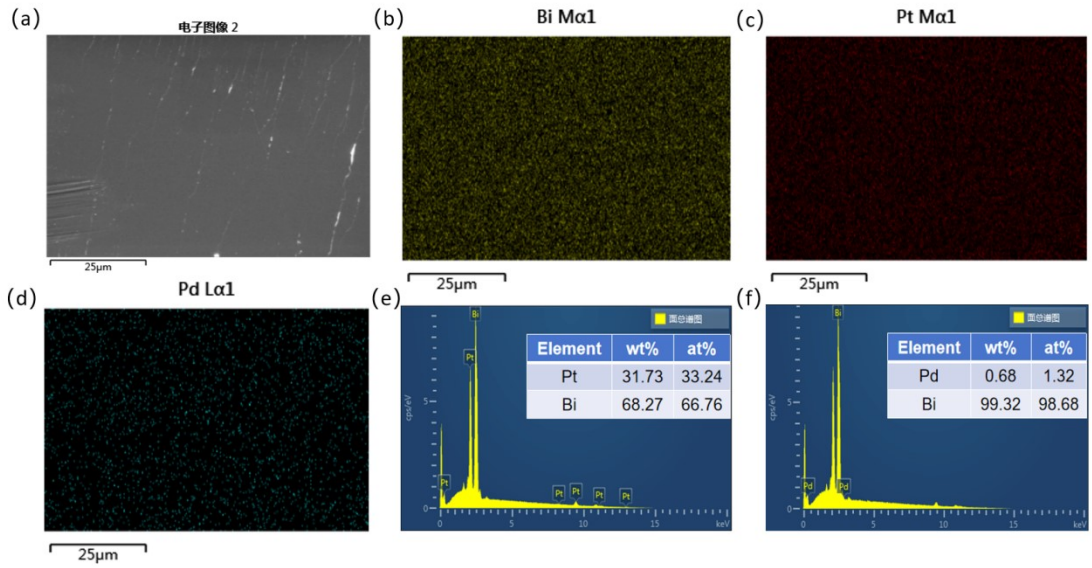

Fig. S7. SEM images of 0.89 at% Pd-$PtBi_2$. EDX spectra of the Pt, Bi elements, and the quantification.EDX spectra of the Pd, Bi elements, and the quantification. Elemental analysis showing the distribution of Bi, Pt, and Pd elements.

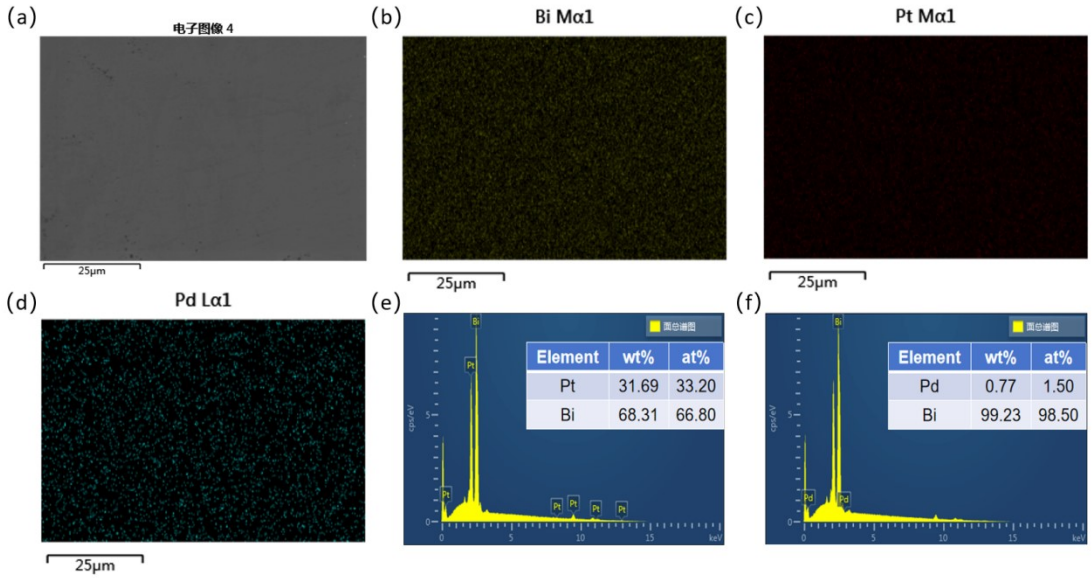

Fig. S8. SEM images of 1.01 at% Pd-$PtBi_2$. EDX spectra of the Pt, Bi elements, and the quantification.EDX spectra of the Pd, Bi elements, and the quantification. Elemental analysis showing the distribution of Bi, Pt, and Pd elements.

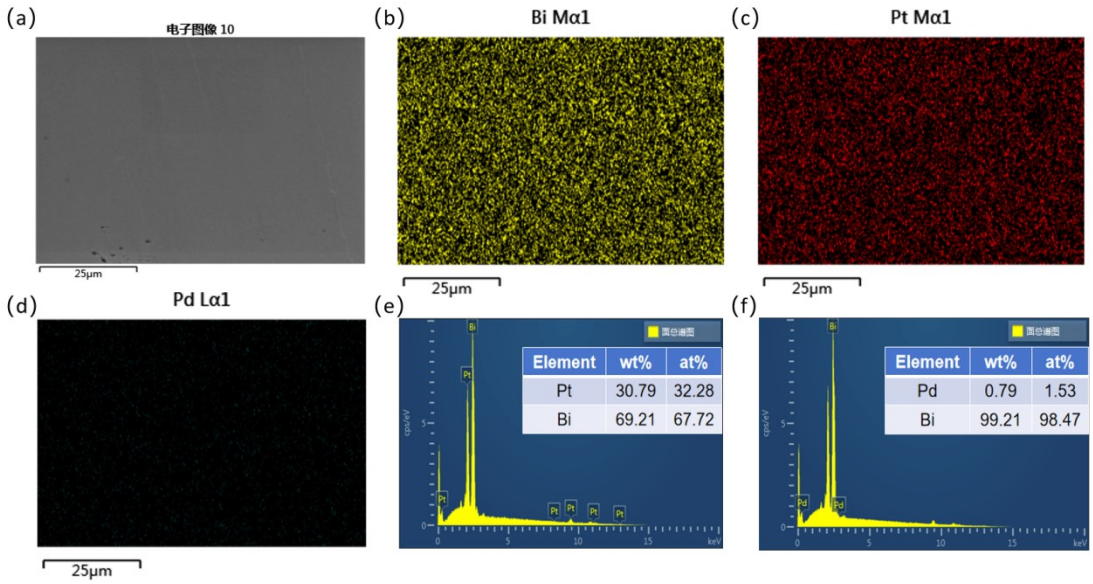

Fig. S9. SEM images of 1.04 at% Pd-$PtBi_2$. EDX spectra of the Pt, Bi elements, and the quantification. EDX spectra of the Pd, Bi elements, and the quantification. Elemental analysis showing the distribution of Bi, Pt, and Pd elements.

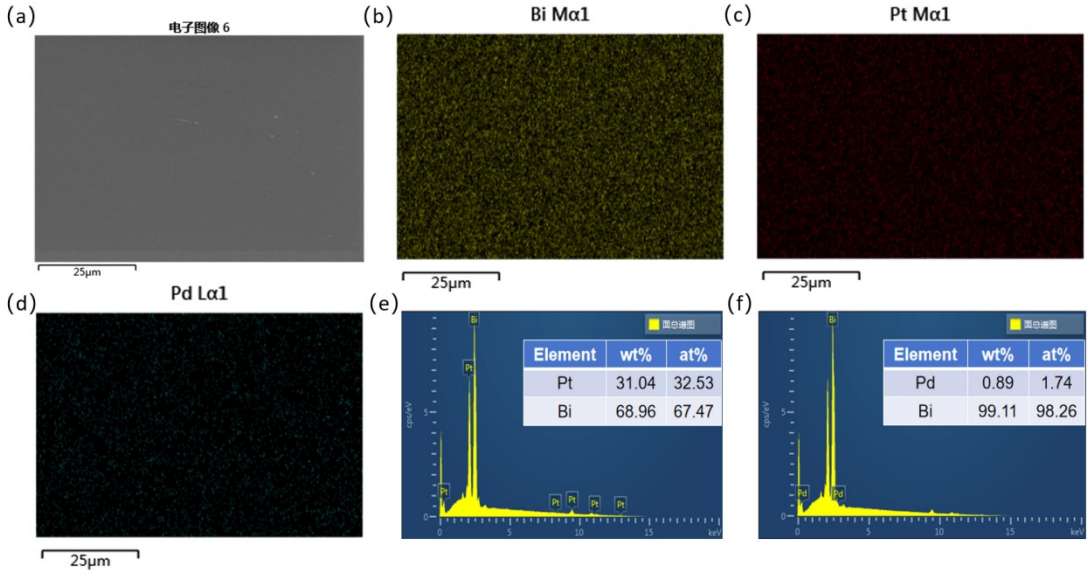

Fig. S10. SEM images of 1.18 at% Pd-$PtBi_2$. EDX spectra of the Pt, Bi elements, and the quantification.EDX spectra of the Pd, Bi elements, and the quantification. Elemental analysis showing the distribution of Bi, Pt, and Pd elements.

Table S2: EDS test atomic ratios and calculated Pd atom occupancies for Pd doped crystals.

Label	Calculated Atomic Ratio Pd : (Pd+Pt+Bi)	EDS Test Atomic Ratio Pt : Bi	EDS Test Atomic Ratio Pd : Bi
0.89 at% Pd-$PtBi_2$	0.0089	33.24 : 66.76	1.32 : 98.68
1.01 at% Pd-$PtBi_2$	0.0101	33.20 : 66.80	1.50 : 98.50
1.04 at% Pd-$PtBi_2$	0.0104	32.28 : 67.72	1.53 : 98.47
1.18 at% Pd-$PtBi_2$	0.0118	32.53 : 67.47	1.74 : 98.26

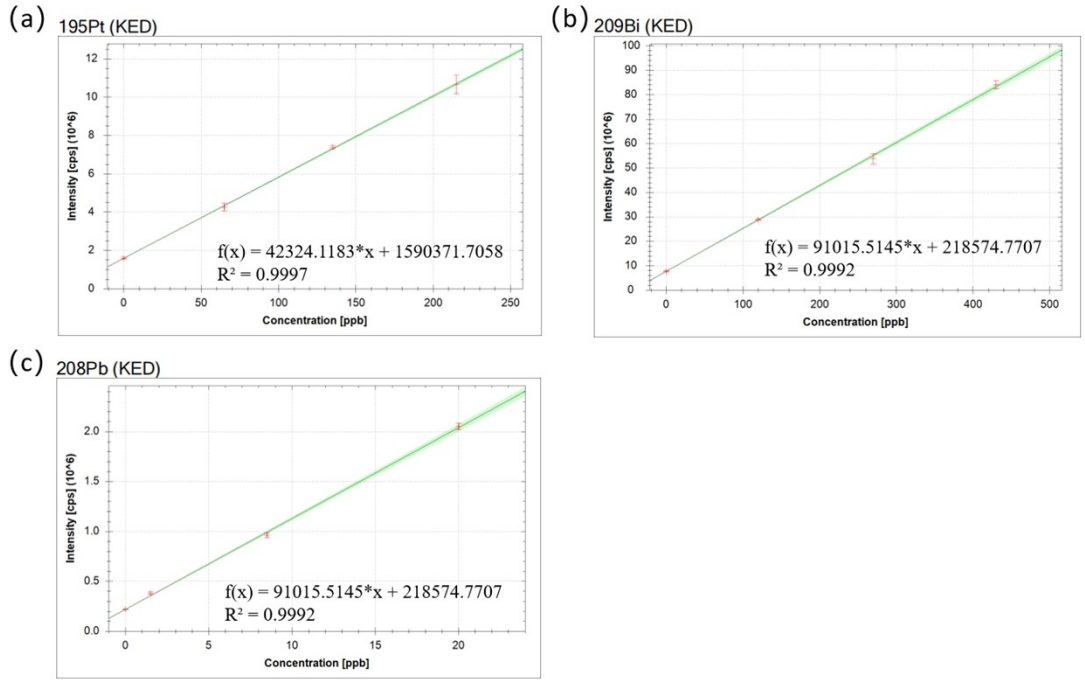

Fig. S11. The calibration curves of (a) Pt, (b) Bi, and (c) Pb elements with ICP-MS.

Table S3: The concentrations of Pt , Pb and Bi elements with ICP-MS.

Label	195Pt (KED) [ppb]	208Pb (KED) [ppb]	209Bi (KED) [ppb]
0.28 at% Pb-$PtBi_2$	73.332	0.759	190.104
0.65 at% Pb-$PtBi_2$	49.099	1.289	146.197
0.88 at% Pb-$PtBi_2$	59.016	1.662	164.164
1.43 at% Pb-$PtBi_2$	71.378	3.783	186.079

The ICP-MS results provided weight ratios of the elements, which we then converted to atomic proportions of the doped Pb elements in the crystals.

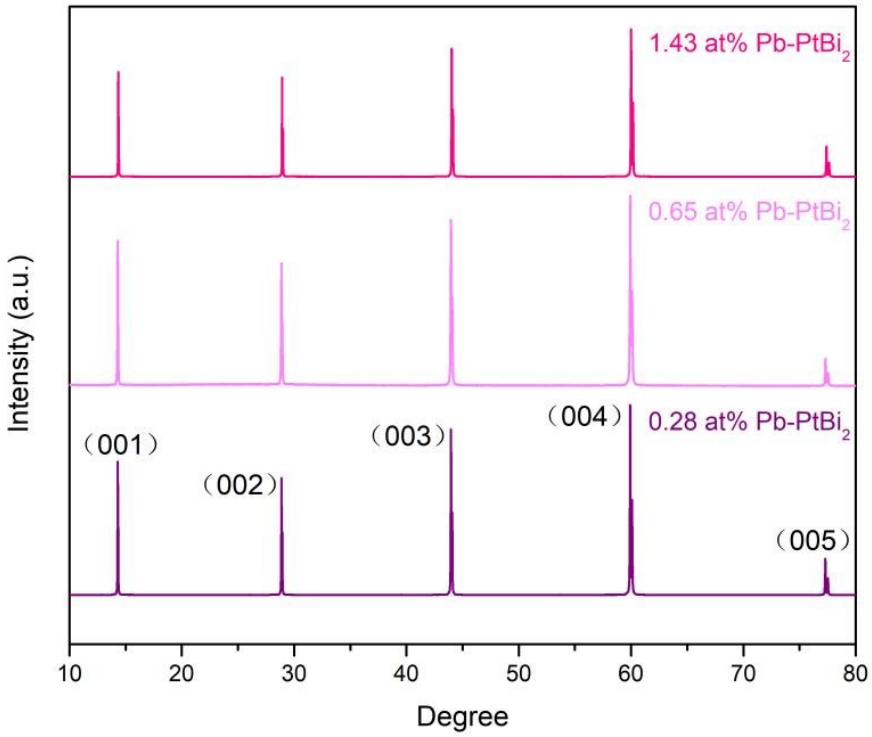

Fig. S12. XRD spectra of Pb $PtBi_2$ with different Pb doping concentrations.

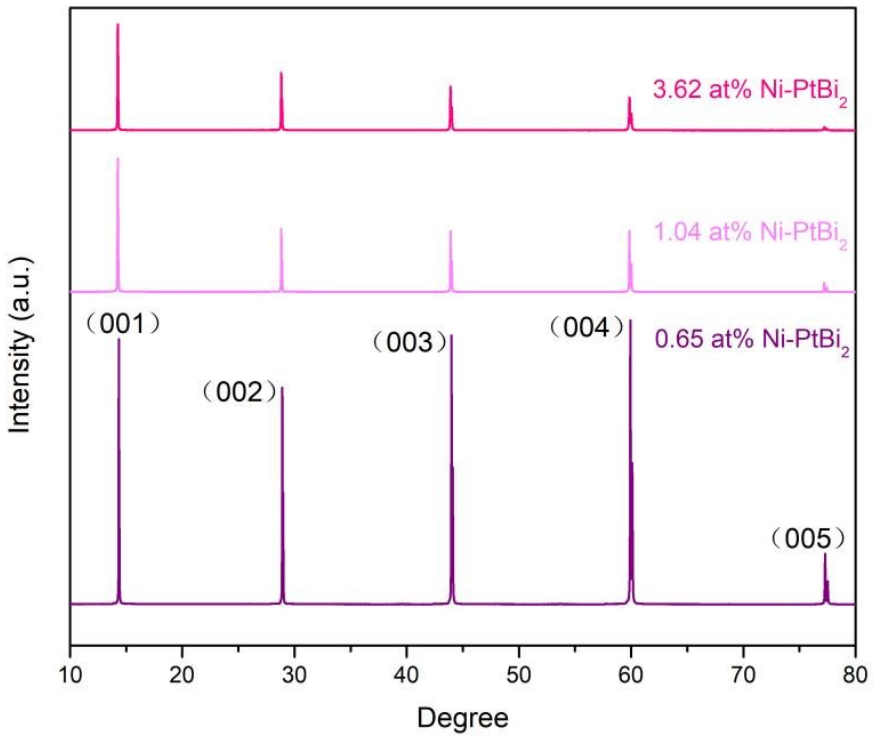

Fig. S13. XRD spectra of Ni-$PtBi_2$ with different Ni doping concentrations.

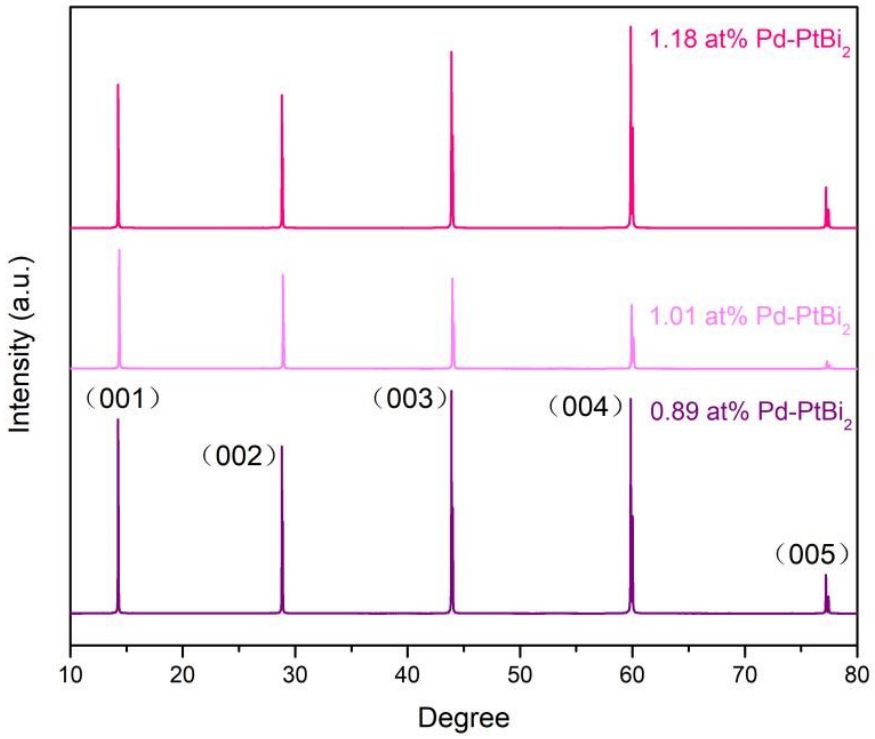

Fig. S14. XRD spectra of Pd-$PtBi_2$ with different Pd doping concentrations.

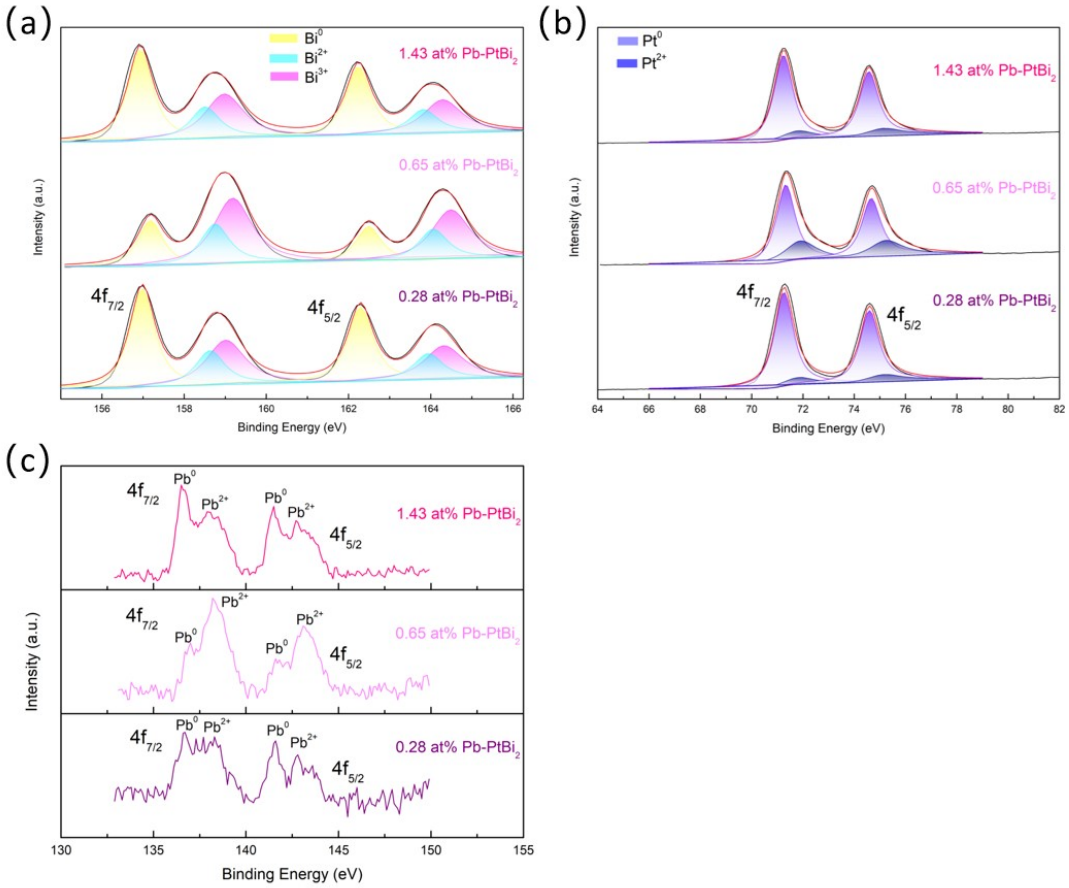

Fig. S15. XPS scanning (a) Bi 4*f*, (b) Pt 4*f*, (c) Pb 4*f* core levels were used to measure Pb-$PtBi_2$ with different Pb doping concentrations.

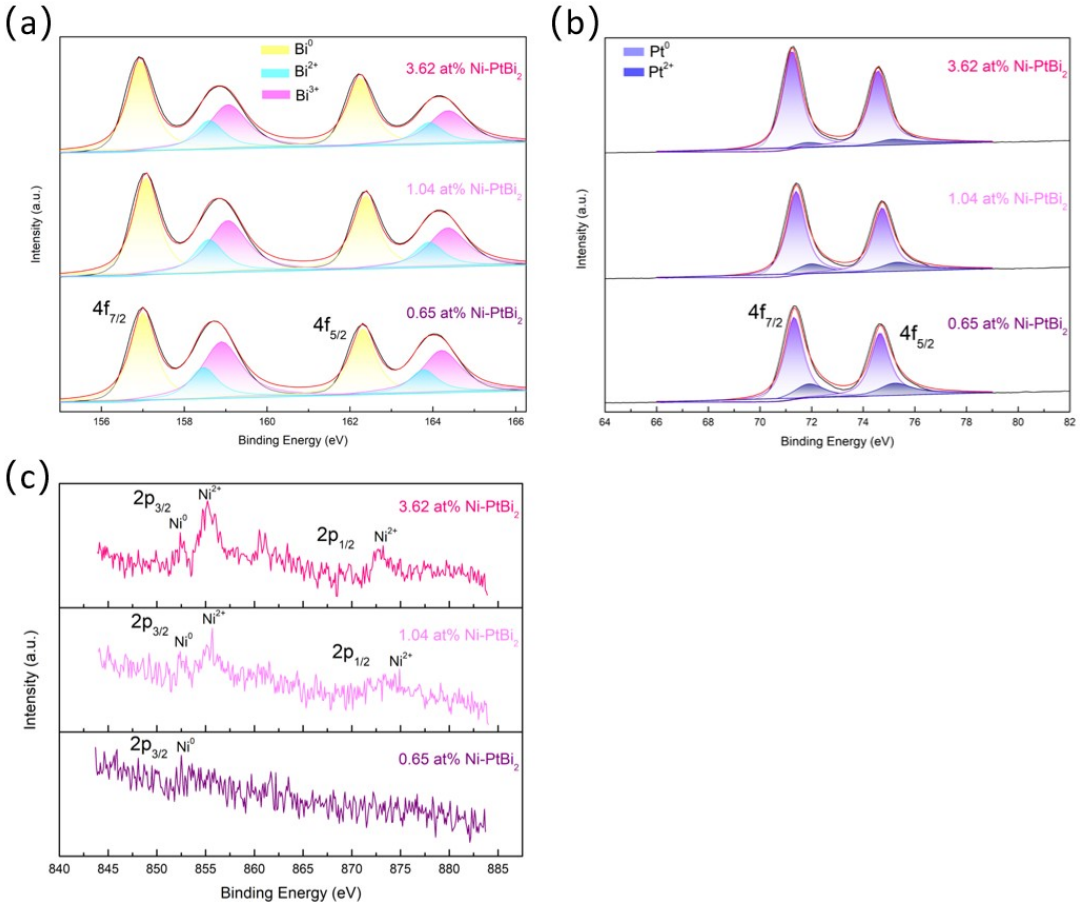

Fig. S16. XPS scanning (a) Bi 4*f*, (b) Pt 4*f*, and (c) Ni 2*p* core levels were used to measure Ni-$PtBi_2$ with different Ni doping concentrations.

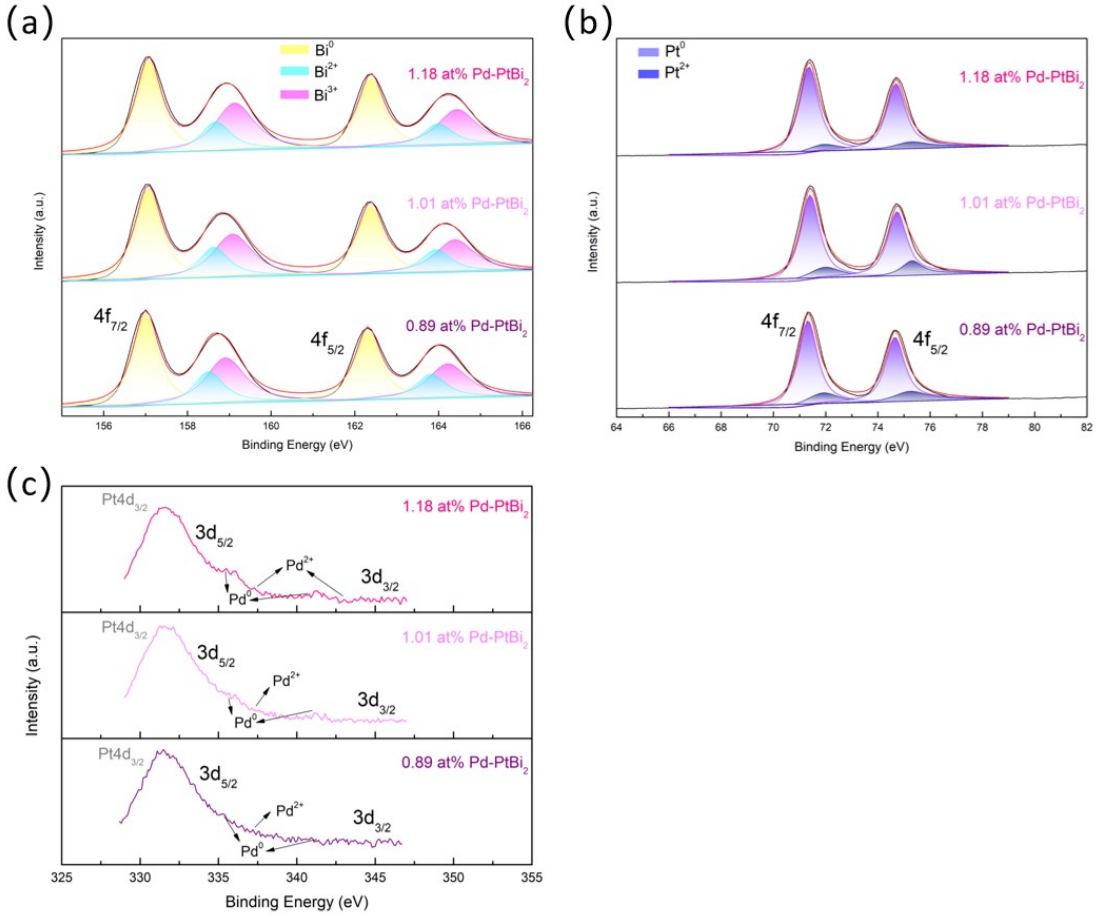

Fig. S17. XPS scanning (a) Bi 4*f*, (b) Pt 4*f*, and (c) Pd 3*d* core levels were used to measure Pd-$PtBi_2$ with different Pd doping concentrations.

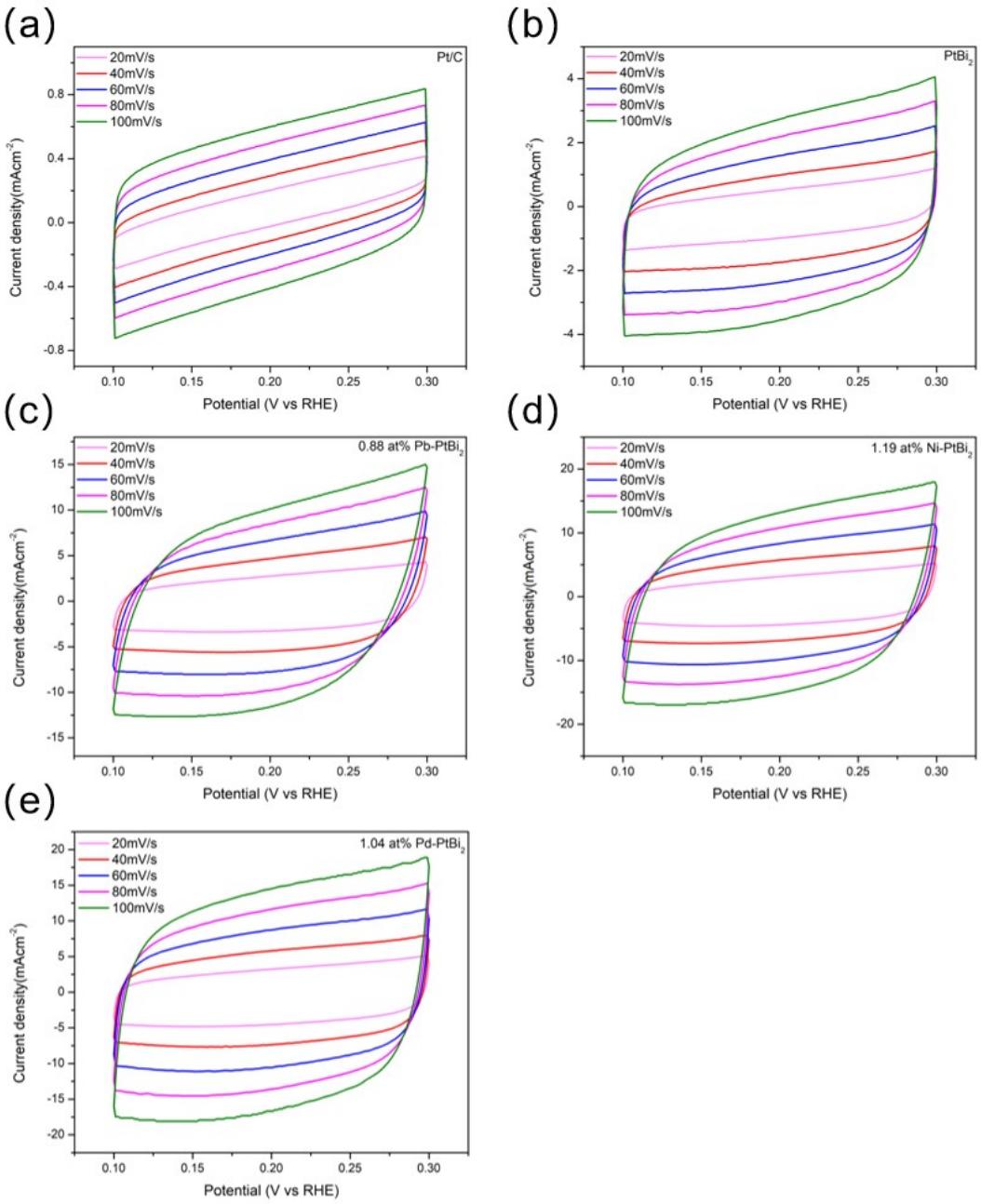

Fig. S18. Shows the cyclic voltammetry curves of samples in 0.5 M H_2SO_4 at different scan rates (20-100 mV/s) (a) Pt/C，(b) $PtBi_2$，(c)0.88 at% Pb-$PtBi_2$，(d) 1.19 at% Ni-$PtBi_2$，(e)1.04 at% Pd-$PtBi_2$.

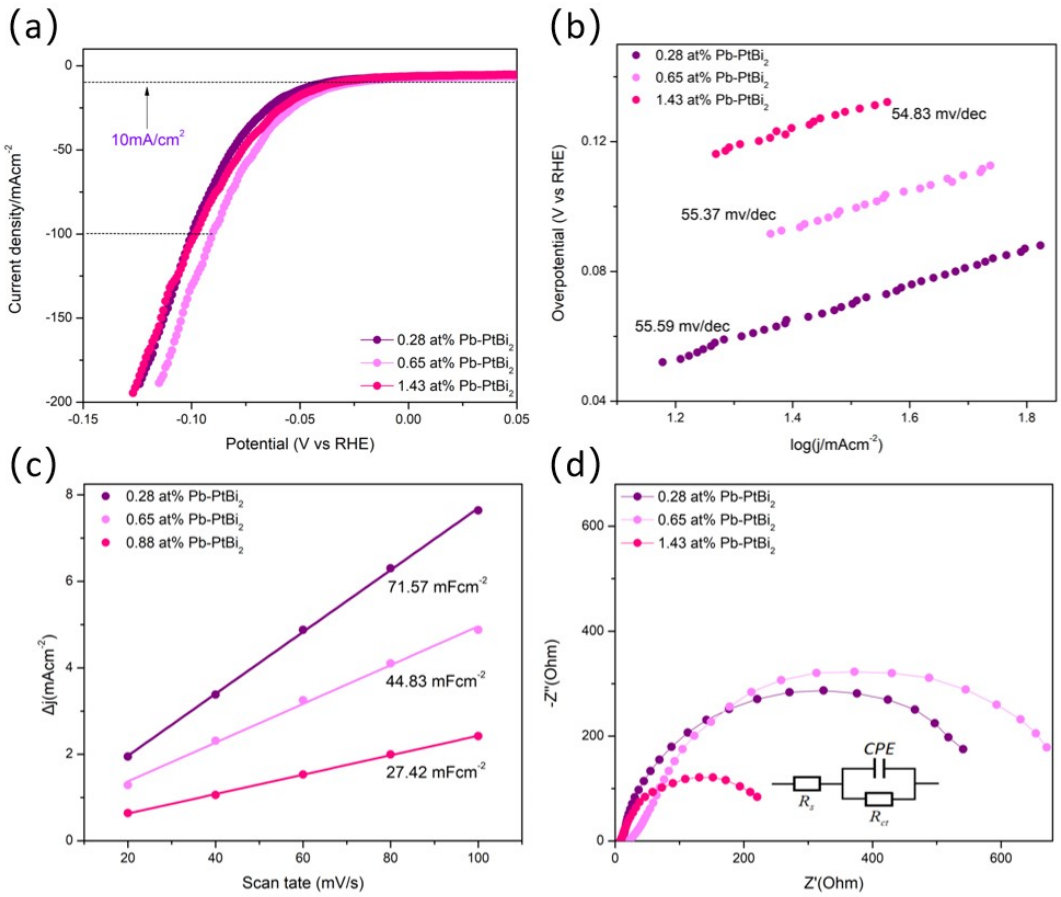

Fig. S19. (a) Linear sweep voltammetry (LSV) polarization curve. (b) Tafel slope. (c) The curve of current density with scanning rate. (d) Nyquist plot obtained from electrochemical impedance spectroscopy (EIS) measurement (illustration: simulated electrochemical equivalent circuit (EEC) of Nyquist plot).

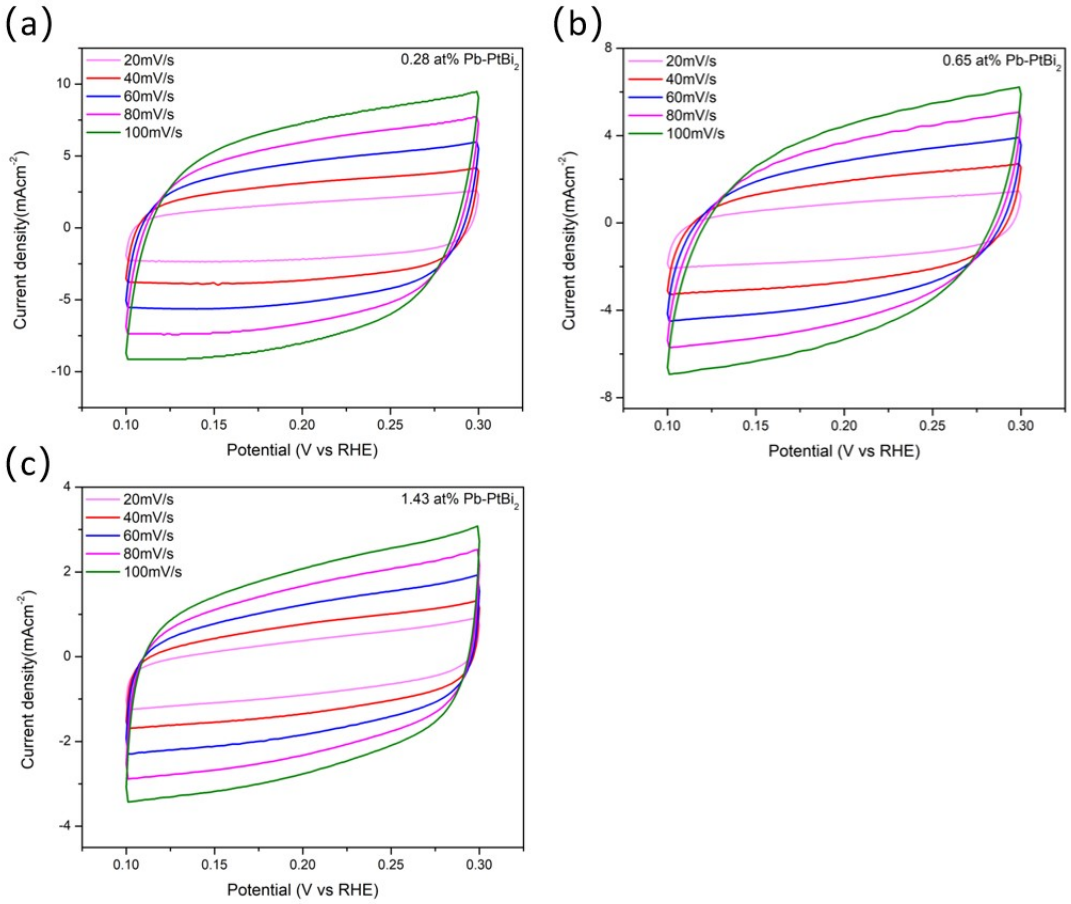

Fig. S20. Shows the cyclic voltammetry curves of samples in 0.5 M H_2SO_4 at different scan rates (20-100 mV/s): (a) 0.28 at% Pb-$PtBi_2$, (b) 0.65 at% Pb-$PtBi_2$, (c) 1.43 at% Pb-$PtBi_2$.

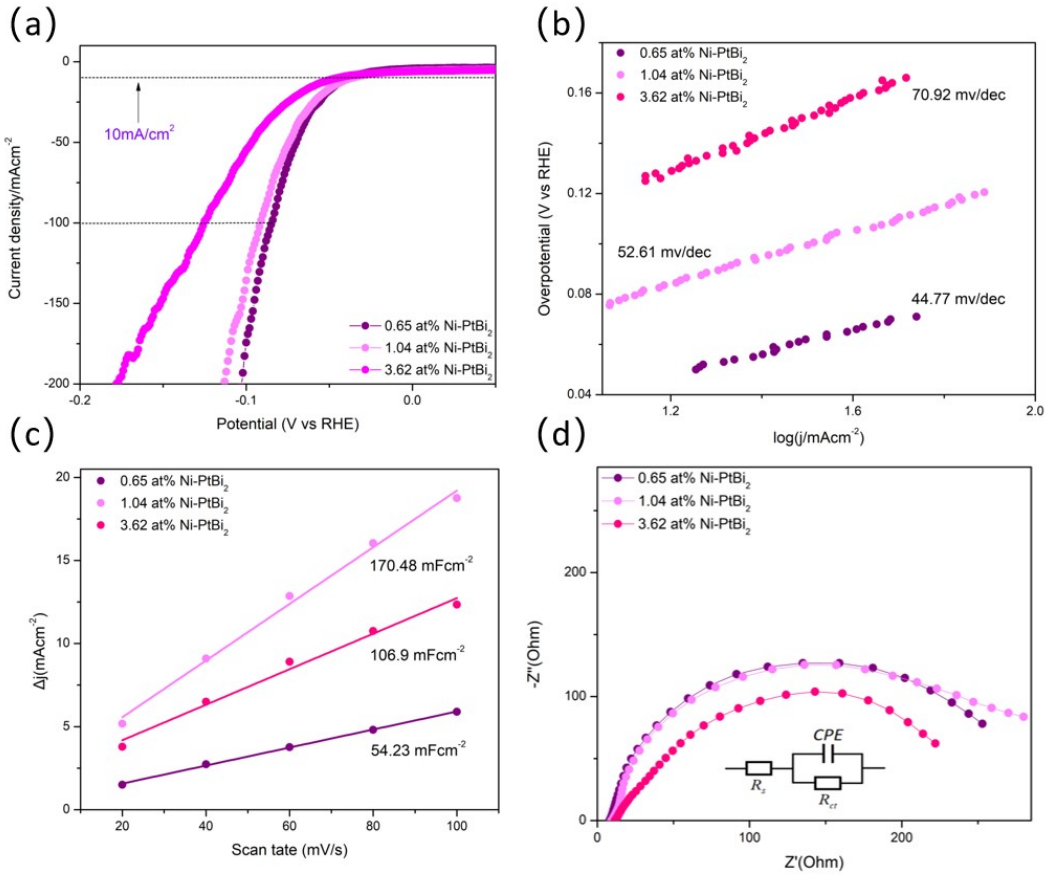

Fig. S21. (a) Linear sweep voltammetry (LSV) polarization curve. (b) Tafel slope. (c) The curve of current density with scanning rate. (d) Nyquist plot obtained from electrochemical impedance spectroscopy (EIS) measurement (illustration: simulated electrochemical equivalent circuit (EEC) of Nyquist plot).

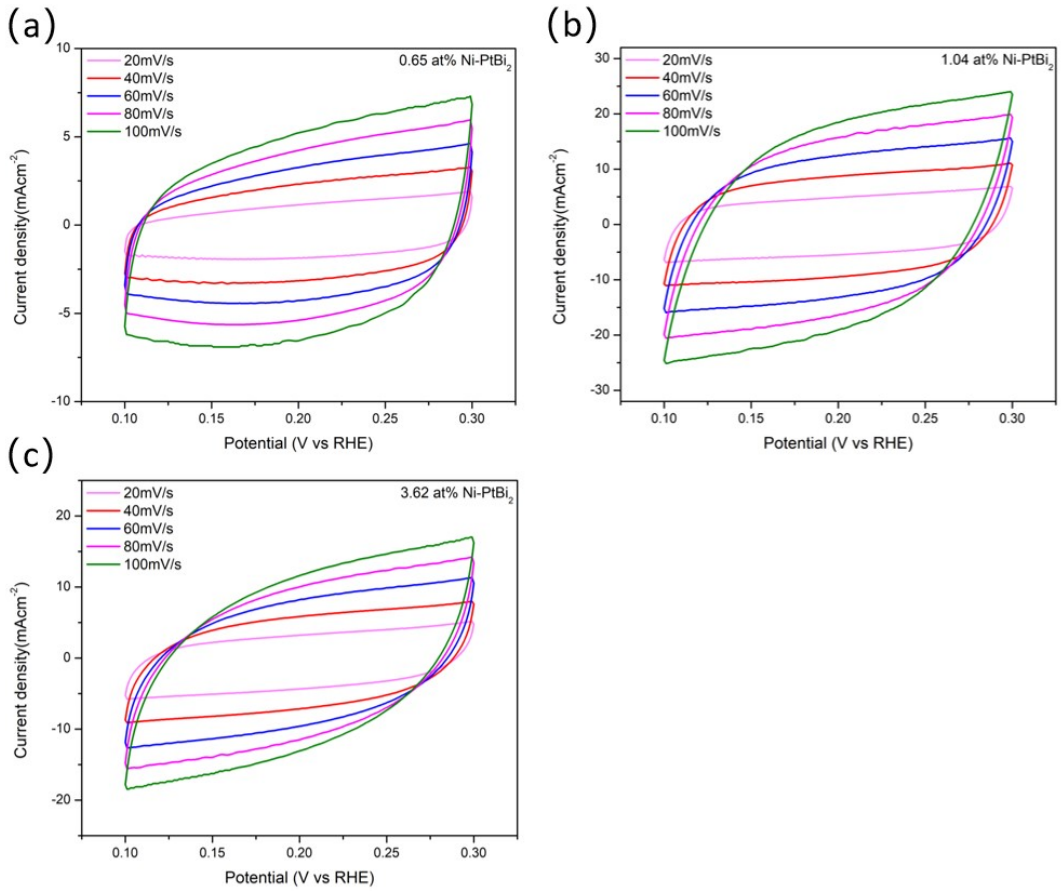

Fig. S22. Shows the cyclic voltammetry curves of samples in 0.5 M H_2SO_4 at different scan rates (20-100 mV/s): (a) 0.65 at% Ni-$PtBi_2$, (b) 1.04 at% Ni-$PtBi_2$, (c) 3.62 at% Ni-$PtBi_2$.

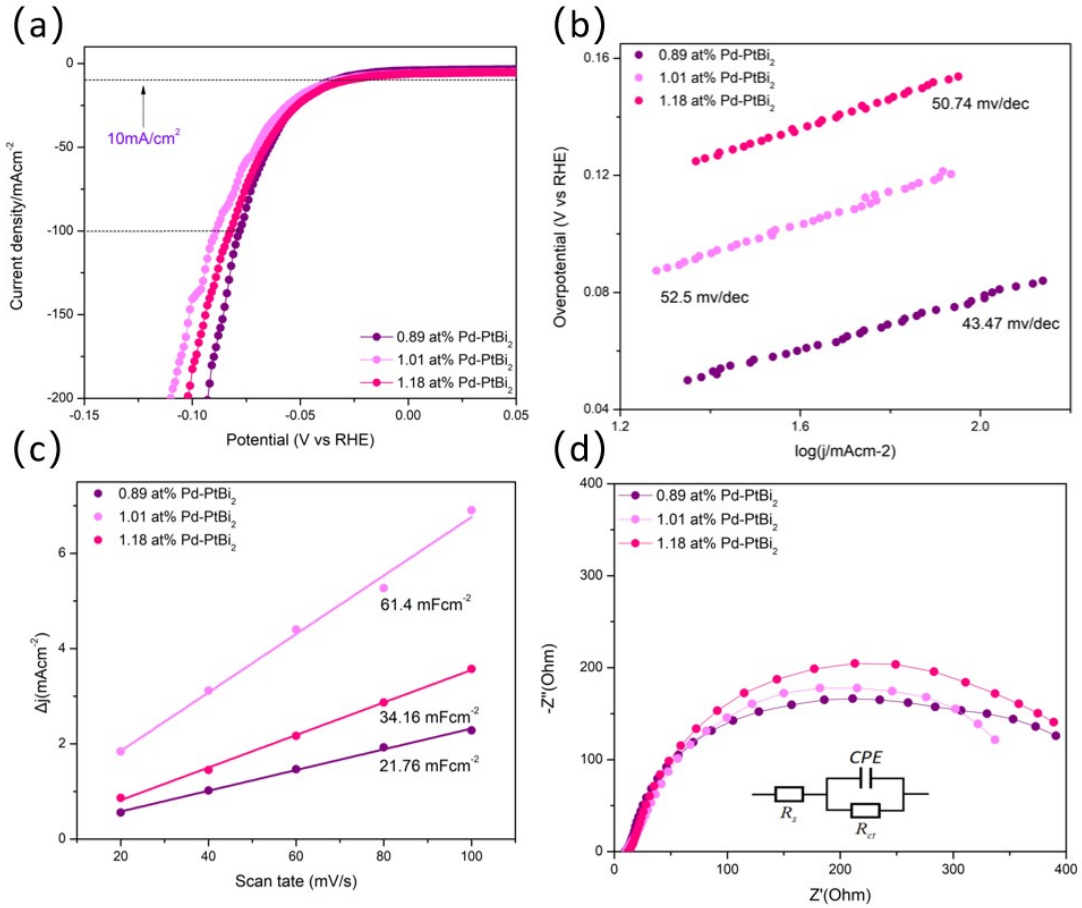

Fig. S23. (a) Linear sweep voltammetry (LSV) polarization curve. (b) Tafel slope. (c) The curve of current density with scanning rate. (d) Nyquist plot obtained from electrochemical impedance spectroscopy (EIS) measurement (illustration: simulated electrochemical equivalent circuit (EEC) of Nyquist plot).

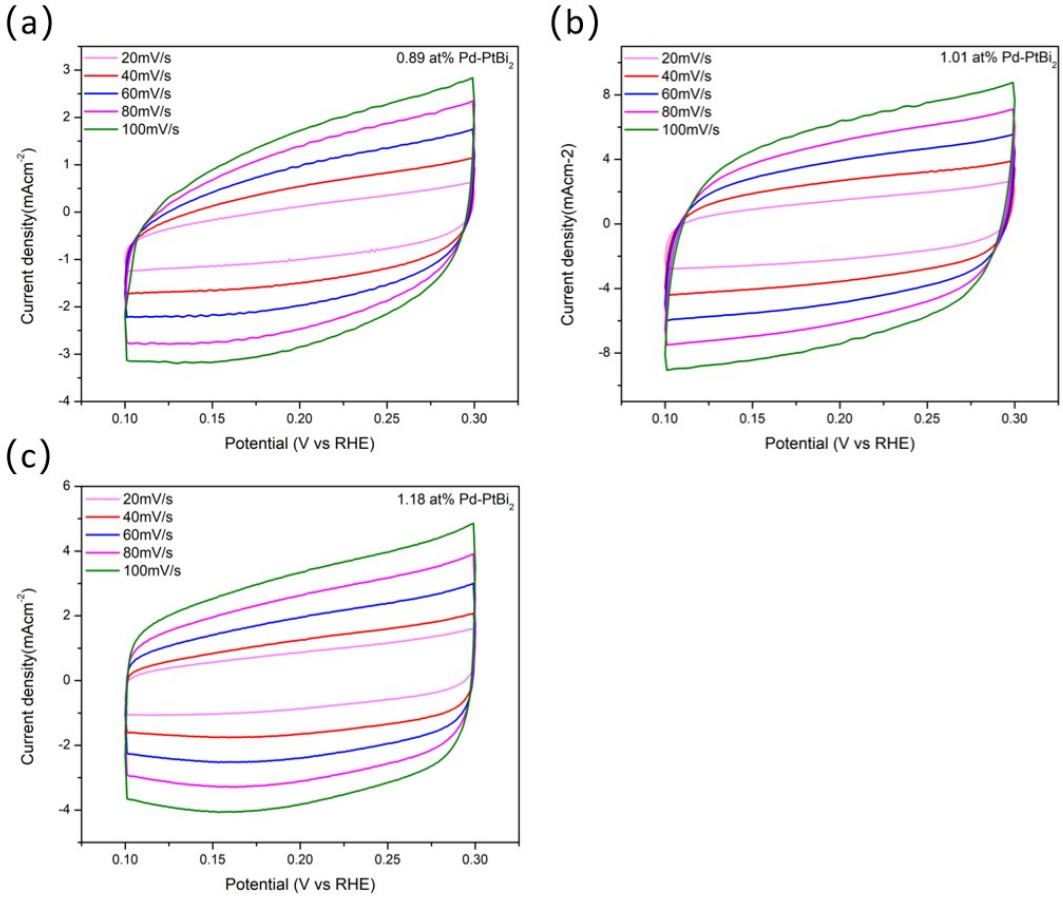

Fig. S24. Shows the cyclic voltammetry curves of samples in 0.5 M H_2SO_4 at different scan rates (20-100 mV/s): (a) 0.89 at% Pd-$PtBi_2$, (b) 1.01 at% Pd-$PtBi_2$, (c) 1.18 at% Pd-$PtBi_2$.

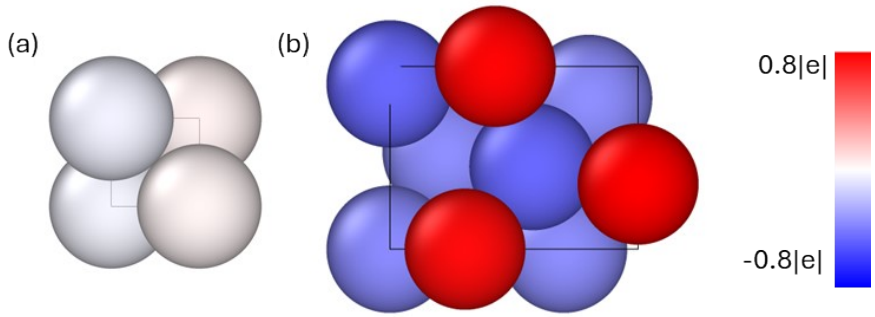

Figure S25. Charges on Pt and Bi in bulk structures with a top view. (a) Pt, (b) $PtBi_2$.

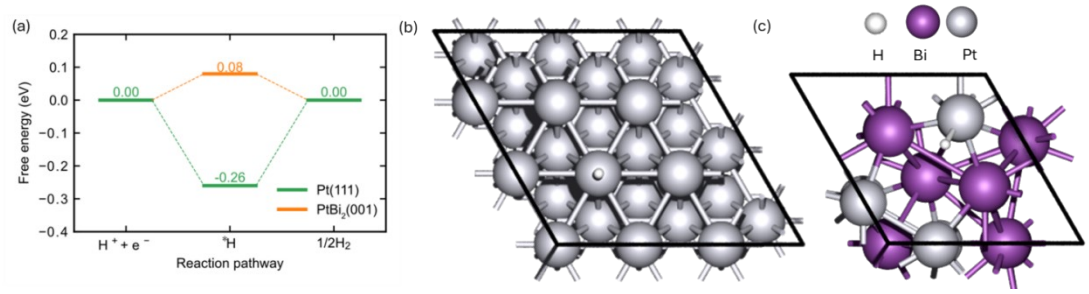

Figure S26. Hydrogen binding energetics and atomic configurations. (a) Calculated free energy surfaces for H adsorption on Pt(111) and PtBi2(001) surfaces. (b,c) Corresponding optimized atomic configurations of H-adsorbed structures.

Table S4. Calculated *d* band center(eV)

surface	*d* band center(eV)
Pt	-2.66
$PtBi_2$	-3.01
Ni-$PtBi_2$	-3.04
Pb-$PtBi_2$	-2.90
Pd-$PtBi_2$	-3.06

Table S5. The HER performance compared with other topological materials electrocatalysts in 0.5 M H_2SO_4.

Electrocatalyst	**Overpotential** (10 mV•cm^{-2})	**Overpotential** (100 mV•cm^{-2})	**Tafel slope** (mV•dec^{-1})	**Stability** Time/CV cycles	Reference
Pt/C	**38**	**107**	**60.8**	**12h**	**This work**
$PtBi_2$	**40**	**96**	**53.6**	**240h**	**This work**
0.88 at% Pb-$PtBi_2$	**39**	**87**	**44.7**	**240h**	**This work**
1.19 at% Ni-$PtBi_2$	**37**	**83**	**44.1**	**240h**	**This work**
1.04 at% Pd-$PtBi_2$	**33**	**80**	**43.8**	**240h**	**This work**
Pt/C	23	~155	35	24h	[1]
$PtTe_2$	109	~260	140	24h	[1]
P-$PtTe_2$	57	~240	88	24h	[1]
A/C-P-$PtTe_2$	28	~148	37	24h	[1]
Ru_3Sn_7	28	-	22	50h	[2]
1T'-MoS_2/CeO_2/rGO	140	-	43	**10000cycles**	[3]
1T'-D/2H WS_2	170	-	40	**10000cycles**	[4]
MoS_2/Bi_2Te_3/STO	248	-	58	20h	[5]
MoS_2/Bi_2Te_3/NF	160	-	66	20h	[5]
1T'-WTe_2 nanoribbon	430	-	57	20h	[6]
Defective WTe_2 nanosheet	251	-	94	26h	[7]

Table S6. The HER performance compared with other Pt-based electrocatalysts in 0.5 M H_2SO_4.

Electrocatalyst	**Overpotential** (10 mV•cm^{-2})	**Overpotential** (100 mV•cm^{-2})	**Tafel slope** (mV•dec^{-1})	**Stability** Time/CV cycles	Reference
Pt/C	**38**	**107**	**60.8**	**12h**	**This work**
$PtBi_2$	**40**	**96**	**53.6**	**240h**	**This work**
0.88 at% Pb-$PtBi_2$	**39**	**87**	**44.7**	**240h**	**This work**
1.19 at% Ni-$PtBi_2$	**37**	**83**	**44.1**	**240h**	**This work**
1.04 at% Pd-$PtBi_2$	**33**	**80**	**43.8**	**240h**	**This work**
Pt/GNs	25	~48	33	**1000cycles**	[8]
Pt-CNTs	41	~210	48	500s	[9]
Pt_{50}-PG	44	134	63	6h	[10]
Pt/f-MWCNTs	43	~90	30	10h	[11]
Pt-Au-Si nanowires	50	~150	24	10h	[12]
$Pt_{0.04}$/Ni-DA	19	-	34	**6000cycles**	[13]
Pt@TiO_2	39	-	42	120h	[14]
Pt/def-WO_3@CFC	42	-	73	70000s	[15]
Pt/GC	56	-	30	3h	[16]
Pt@PCM	105	-	65.3	5h	[17]

1. H. Ma, X. Huang, L. Li, W. Peng, S. Lin, Y. Ding and L. Mai,Boosting the Hydrogen Evolution Reaction Performance of P-Doped PtTe2 Nanocages via Spontaneous Defects Formation,*Small*, 2023, **19**.
2. X. Zhang, L. Wang, M. Li, W. Meng, Y. Liu, X. Dai, G. Liu, Y. Gu, J. Liu and L. Kou,Topological surface state: Universal catalytic descriptor in topological catalysis,*Materials Today*, 2023, **67**, 23-32.
3. K. Nie, X. Qu, D. Gao, B. Li, Y. Yuan, Q. Liu, X. Li, S. Chong and Z. Liu,Engineering Phase Stability of Semimetallic MoS2 Monolayers for Sustainable Electrocatalytic Hydrogen Production,*ACS Applied Materials & Interfaces*, 2022, **14**, 19847-19856.
4. L. Wang, G. Zhou, H. Luo, Q. Zhang, J. Wang, C. Zhao, A. M. Rao, B. Xu and B. Lu,Enhancing catalytic activity of tungsten disulfide through topology,*Applied Catalysis B: Environmental*, 2019, **256**.
5. G. Li, J. Huang, Q. Yang, L. Zhang, Q. Mu, Y. Sun, S. Parkin, K. Chang and C. Felser,MoS2 on topological insulator Bi2Te3 thin films: Activation of the basal plane for hydrogen reduction,*Journal of Energy Chemistry*, 2021, **62**, 516-522.
6. J. Li, M. Hong, L. Sun, W. Zhang, H. Shu and H. Chang,Enhanced Electrocatalytic Hydrogen Evolution from Large-Scale, Facile-Prepared, Highly Crystalline WTe2 Nanoribbons with Weyl Semimetallic Phase,*ACS Applied Materials & Interfaces*, 2017, **10**, 458-467.
7. X. Wang, J. Wang, B. Wei, N. Zhang, J. Xu, H. Miao, L. Liu, C. Su, Y. Li and Z. Wang,Plasma tailoring in WTe2 nanosheets for efficiently boosting hydrogen evolution reaction,*Journal of Materials Science & Technology*, 2021, **78**, 170-175.
8. X. Yan, H. Li, J. Sun, P. Liu, H. Zhang, B. Xu and J. Guo,Pt nanoparticles decorated high-defective graphene nanospheres as highly efficient catalysts for the hydrogen evolution reaction,*Carbon*, 2018, **137**, 405-410.
9. W. Zhong, W. Tu, Z. Wang, Z. Lin, A. Xu, X. Ye, D. Chen and B. Xiao,Ultralow-temperature assisted synthesis of single platinum atoms anchored on carbon nanotubes for efficiently electrocatalytic acidic hydrogen evolution,*Journal of Energy Chemistry*, 2020, **51**, 280-284.
10. L.-C. Balint, I. Hulka and A. Kellenberger,Pencil Graphite Electrodes Decorated with Platinum Nanoparticles as Efficient Electrocatalysts for Hydrogen Evolution Reaction,*Materials*, 2021, **15**.
11. J. Ji, Y. Zhang, L. Tang, C. Liu, X. Gao, M. Sun, J. Zheng, M. Ling, C. Liang and Z. Lin,Platinum single-atom and cluster anchored on functionalized MWCNTs with ultrahigh mass efficiency for electrocatalytic hydrogen evolution,*Nano Energy*, 2019, **63**.
12. B. Jiang, Z. Tang, F. Liao, H. Lin, S. Lu, Y. Li and M. Shao,Powerful synergy: efficient Pt–Au–Si nanocomposites as state-of-the-art catalysts for electrochemical hydrogen evolution,*J. Mater. Chem. A*, 2017, **5**, 21903-21908.
13. Y. Peng, K. Ma, T. Xie, J. Du, L. Zheng, F. Zhang, X. Fan, W. Peng, J. Ji and Y. Li,Tunable Pt–Ni Interaction Induced Construction of Disparate Atomically Dispersed Pt Sites for Acidic Hydrogen Evolution,*ACS Applied Materials & Interfaces*, 2023, **15**, 27089-27098.
14. S. Cho, G. Yim, J. Koh, H. Jang and J. T. Park,One-pot synthesis of Pt@TiO2 core-shell nanoparticles for stable hydrogen evolution reaction in acidic and alkaline media,*Materials Today Chemistry*, 2023, **32**.

15. H. Tian, X. Cui, L. Zeng, L. Su, Y. Song and J. Shi,Oxygen vacancy-assisted hydrogen evolution reaction of the Pt/WO3 electrocatalyst,*Journal of Materials Chemistry A*, 2019, **7**, 6285-6293.
16. L. Rakočević, J. Golubović, D. Vasiljević Radović, V. Rajić and S. Štrbac,A comparative study of hydrogen evolution on Pt/GC and Pt/GNPs in acid solution,*International Journal of Hydrogen Energy*, 2024, **51**, 1240-1254.
17. H. Zhang, P. An, W. Zhou, B. Y. Guan, P. Zhang, J. Dong and X. W. Lou,Dynamic traction of lattice-confined platinum atoms into mesoporous carbon matrix for hydrogen evolution reaction,*Science Advances*, **4**, eaao6657.